

AIRCRAFT LOADS – AN IMPORTANT TASK FROM PRE-DESIGN TO LOADS FLIGHT TESTING

T. Klimmek¹, P. Ohme², P. D. Ciampa³, and V. Handojo¹,
DLR, German Aerospace Center,

¹Institute of Aeroelasticity, 37073 Göttingen, Germany, ²Institute for Flight Systems, 38108 Braunschweig, Germany, ³Institute of Air Transportation Systems, 21079 Hamburg

Summary

The estimation of loads acting on an aircraft structure is an indispensable task ranging from conceptual, preliminary, and detail design to loads flight testing when an aircraft is already in service. Work package 4 of the DLR project iLOADS covers the range broadly. Physics-based loads and aerodynamic performance analysis methods in pre-design are presented using a parameterized and automatized process nested in an overall aircraft design loop. Such process can be used for conventional and unconventional configurations. Covering the complete design process, a parametric set-up for structural modeling, estimation of loads and loads flight testing for the DLR HALO, a modified Gulfstream G550, is also shown. Finally the in-flight system identification activities including flight tests for the DLR Discus-2c are described.

1. INTRODUCTION

Aircraft loads analysis is an important engineering discipline playing a major role from the first sketch of a new aircraft until the decommissioning. A proper estimation of the loads in the design process is reflected by the structure withstanding the loads and essentially by the structural weight that is about to be minimized. The monitoring of the loads acting on the structure when the aircraft is in service is as well significant. On the one hand the measured loads are compared to the predicted loads and on the other hand the loads data can be used to estimate the real lifetime of an aircraft mainly driven by fatigue.

A big portion of such a wide range is covered by the research activities at DLR within work package 4 of the DLR project iLOADS (2013-2016). The project iLOADS is focused on the loads process and has the task to gather almost all research activities respectively research institute, being part of or closely connected to the aircraft loads process. A more detailed description of the project is given in [10]. In work package 4 of iLOADS a wide range of loads analysis and measurement is covered from conceptual design, and loads analysis for a complete aircraft to loads flight testing.

Few publications are available where a comprehensive survey regarding loads analysis is presented. The books from Lomax [11], as well as the one from Wright and Cooper [16], are describing various loads analysis methods for almost all load types that have to be considered in aircraft design. Niu presents in his book [13] on airframe stress analysis besides basic loads analysis methods, the interfaces and the interdependencies of the loads group to the groups and departments of a typical aircraft manufacture.

The estimation of loads acting on an aircraft is an important task already at early steps of the design, because the structural mass, always to be minimized, is the result of a structural sizing with the assumed design loads. In conceptual design normally only statistics based

or analytical methods are applied, because knowledge of the design of a new aircraft is rare or wide range parameter studies require fast analyses methods [15]. To improve the overall aircraft design (OAD) process physics based methods for aeroelastic loads analysis and the aerodynamic performance assessment of the flexible structure are integrated in an OAD process shown in chapter 2.

The loads analysis for the complete aircraft is shown for the DLR HALO, a slightly modified G550 from Gulfstream Aerospace Company (GAC) to be used for atmospheric research. The DLR HALO lacks an applicable structural model for loads analysis. Such structural models are normally company confidential and consequently publicly not available. Therefore, one task of iLOADS was to set up a structural model for the DLR HALO to enable loads analysis. The process, wherein limited available data from GAC were used, and the results of selected load cases is presented in chapter 3.

Regarding the measurement of flight loads two DLR aircraft were considered, on the one hand again the DLR HALO, with the focus on the interface loads between the stores and the wing, and on the other hand the DLR Discus 2c, where the measurement of loads is part of an overall system identification.

Like military aircraft the DLR HALO is also designed to carry wing stores, for the DLR HALO to be used for atmospheric research. As the manufacture sets limiting loads between the stores and the aircraft, it has to be shown in advance for new stores or already certified stores with another mass and center of gravity that the interface loads are not exceeded. To improve the capabilities of DLR to support such certification process, the flight tests were done (see chapter 4).

Finally, as part of a comprehensive system identification flight test of the sailplane DLR Discus-2c were executed. The measurement equipment is shown, as well first results, that are planned to be used to set up a loads model purely based on flight-test (see chapter 5).

2. LOADS ANALYSIS IN PRE-DESIGN

2.1. Loads in Overall Aircraft Design

The early aircraft development stages focus on the feasibility and on the assessment of the overall performance of the investigated configurations. During the pre-design stages design details are typically not available, and the overall aircraft synthesis relies on the specification of TLAR (Top Level Aircraft Requirements), such as transportation mission and operational constraints, and provides as output the overall aircraft parameters, such as MTOW (Maximum Take Off Weight), mission fuel consumption, etc.[21].

Despite the large impact of loads on the aircraft performance, conceptual overall aircraft design (OAD) methodologies are mainly based on statistical data. At best, the airframe's loads carrying components are estimated by empirical relations or database available from previous designs rather than by incorporating physics-based analyses. Furthermore, at the early stages the estimation of the relevant load cases includes conservative allowances and safety margins for the structural design in order to guarantee the structural integrity. This rather conventional design approach usually adds an "aeroelastic penalty" [4] to the final designed structures, which may be unveiled only at the later phases of the development. Flexibility effects on the performance are also conventionally not included during the pre-design phases of the investigations. However, with the increasing efficiency of the structural design concepts, the importance of flexible effects is significantly growing. Those effects need to be properly accounted from the beginning of the aircraft development in order to minimize expensive redesign activities or the degradation of the prospected performance. The recent advancement in computational performance and simulation capabilities provide accessibility to time efficient physics based models which could be adopted from the beginning of the developments.

The integration of such models in overall aircraft synthesis process is here presented, and it is part of an overall framework aiming to enhance the aircraft pre-design activities of conventional and unconventional configurations. Focus in on accounting a low fidelity loads analysis process and investigate the impact it has on the early design stages. The full automation of such a process is a key feature, since at the pre-design stages large trade-off studies, and design of experiments are expected to be performed.

2.2. Multi-fidelity Loads Process

A fully automated OAD multi-fidelity process is assembled within the iLOADS Project. The process is characterized by 3 phases, with focus on the aero-structural design modules which are used to investigate how a physics loads analysis process may impact the overall aircraft synthesis and the designed performance. A representation schema of the process is shown in FIGURE 1.

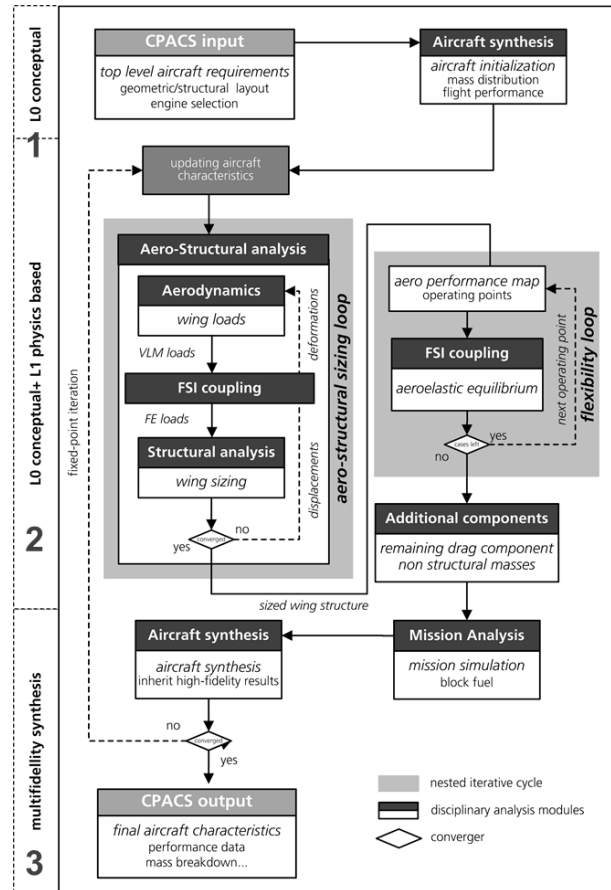


FIGURE 1. Multi-Fidelity Loads Process

The first phase is the initialization of the aircraft, labeled in the schema as "L0 conceptual". The initialization step provides the first full aircraft synthesis for a given set of TLAR. The synthesis is provided by a conceptual aircraft synthesis module, whose formulations are based on typical aircraft design methodologies. The output is a representation of synthesized aircraft, and its performance, such as the aircraft design masses, mission fuel as shown in FIGURE 2. Further, the solution is augmented by additional features in order to enable to progress the design solution to the next phase which is using low fidelity physics based analysis modules. Examples of enhanced details are the initialization of a representative wing internal structural topology, the three dimensional shape of the aircraft components.

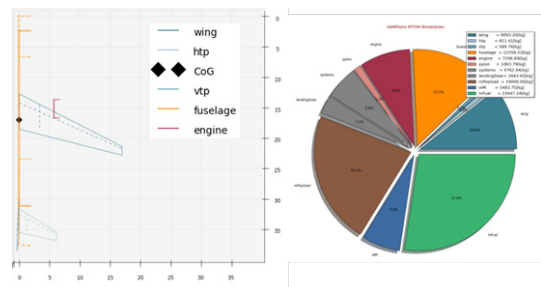


FIGURE 2. Initialization Phase – Conceptual L0

Thereafter, the solution is forward to the second phase, in which the physics based low fidelity modules analyze the initialized aircraft. The second phase is labeled in the schema as “L0 conceptual + L1 physics based”. Although the approach may be extended to comprise all the aircraft disciplines, in the current process the focus is on the aero-structural analysis and design modules. The aim is to provide a more accurate representation of the physics behaviors with respect to the previous conceptual phase. At this stage two main effects are identified and investigated by making use of the modules:

1. The **aero-structural sizing loop**: in this sub-process the wings primary structural components are sized with respect to a selected set of critical loads cases. The output consists in the sized structures and the corresponding structural masses.
2. The **flexibility loop**: the aircraft performance (e.g. the aerodynamics polar) are evaluated considering the flexibility effects of the airframe, and a thus evaluating the static aeroelastic equilibrium for each flow condition. The FSI coupling is taken into account to determine the lift and drag coefficients of the aircraft, for relevant combinations of angle of attack, Mach and Reynolds number. Hence, the updated aircraft aerodynamic performance, corrected by the flexibility effects

For both the effects, an available VLM based module is used to estimate the aerodynamics efficiency at various conditions of the flight envelope, and to provide the aerodynamics loading distribution on the lifting surfaces as resulting from the critical design maneuvers. The structural representation relies on a simplified Finite Element (FE) formulation for the modeling, analysis and post-processing of the aircraft primary structures (i.e. explicit wing-box modeling), in order to determine the displacements and the stress fields of the aircraft under multiple load cases. A number of sizing strategies, such fully stress design, and flexural buckling criteria, are implemented for the dimensioning of the selected primary structures. In order to account for the aircraft flexibility effects, the fluid-structure interactions (FSI) need to be considered in the aero-structural analysis and sizing process. The aero-structural coupling is implemented by first mapping the aerodynamics forces on to the structural model, and then transferring the computed displacements on the structural nodes to the aerodynamic geometry. Since the disciplinary modules are loosely coupled, the coupling schemes implemented are based on MLS\RBF for the forces-displacements transfers in both the sizing and the flexibility loops [2].

FIGURE 3 shows the disciplinary models generated by the analysis tools, namely the aerodynamics VLM lattice for the lifting surfaces, and the FE beam model of the aircraft. The nodal deflections are also shown for the main wing, under the critical sizing load case. Figure 3 shows the structural model with the aerodynamics loads on the FE nodes of the main wing, as resulting from the mapping schema from the VLM lattice to the structural grid, and the structural nodal displacements of the FE model and the propagation of the displacements on the geometry, via mesh deformation techniques available in the module, applied directly on the initial geometry, and on the disciplinary VLM grid

Thereafter, a mission analysis is performed, and an updated value of the mission fuel is calculated. Respect to the mission fuel calculated in the first phase, the updated amount account for the updates structural masses and flexible performance which are provided by the physics based simulations.

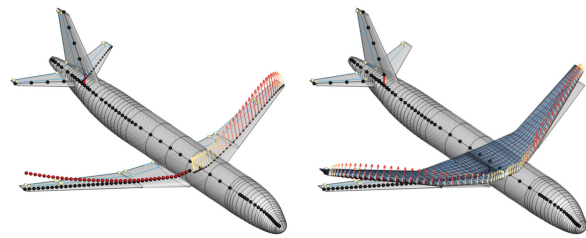


FIGURE 3. Multi-fidelity, physics based disciplinary modules

The third stage is here labeled as “multi-fidelity synthesis”. All the updated aircraft characteristics are used to update the OAD synthesis and the overall estimation of the performance. In this phase the conceptual design tool is still the one called by the initialization phase, but values calculated from the physics based modules replace the conceptual estimations. The updated synthesis will produce new overall aircraft design values (MTOM), an updated initialized aircraft become available. The solution can be progressed once more to the physics based phase. Hence, the full multi-fidelity cycle is iteratively repeated via the fixed point iteration architecture, until the convergence of the aircraft design masses.

The integration of the described process is a workflow assembled in RCE environment [6] [18], whose corresponding workflow is shown in FIGURE 4, and the transfer of data between modules is via the CPACS format [5]. All the models generations, analysis and design are fully automated. Further, the process may be employed to analyze any type of configuration described in the CPACS file (within the limits of the physics formulation behind the modules). Examples of models generated by the system for unconventional aircraft are shown in FIGURE 5.

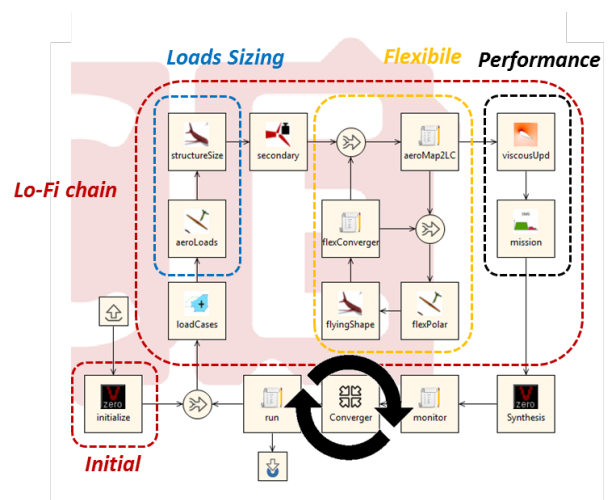


FIGURE 4. Multi-Fidelity Loads Process RCE Workflow

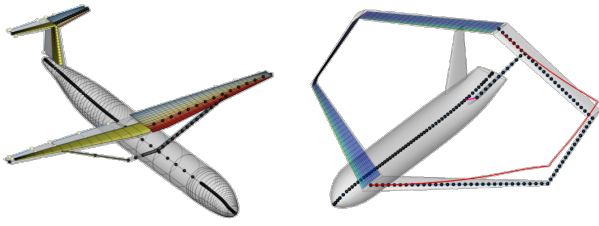


FIGURE 5. Disciplinary modules automation for unconventional CPACS configurations

2.3. Use case

A conventional transportation aircraft configuration, the DLR D-150, is selected as use case of the multi-fidelity process described in the previous section. Among the others, the main mission's requirements are a design range of 3500 nm, at Mach 0.78, with 150 passengers. Although the set of TLAR is sufficient for the conceptual synthesis, additional tools' specific inputs are required for the other disciplinary modules, e.g. materials allocation, selection of the propulsion system technologies. The process described in the previous section can be executed with the following modalities: only conceptual design process (L0 level), conceptual and physics based (multi-fidelity L0 + L1 level) with and without flexibility effects. In this, way the designer can tailor the process according to required level of accuracy and/or computational speed.

On the conventional aircraft use case two incremental studies are performed. The first study focus on the sizing loop, and the sensitivity it has on the OAD synthesis. The comparison is between the synthesis results from the only conceptual process, against the multi-fidelity synthesis presented (but without the flexibility loop at first). Further, the multi-fidelity approach is performed multiple times with a varying number of critical loads cases to be included in the loads process for the structural sizing task. The synthesis results are also compared against the reference data available for the aircraft model, and additionally against a previous internal project VAMP [12], in which the same aircraft was design by making use of higher fidelity disciplines. TAB 1 and TAB 2 presents the comparison of the aircraft synthesis design masses and performance for all the mentioned cases.

TAB 1. D150 synthesis comparison

Use Case D-150	Ref.data	VAMP ^{1, 2}	Conceptual ¹
MTOM [kg]	73500	-0.11%	79282
Fuel Mass [kg]	-	-	17261
OEM [kg]	40925.9	-1.73%	43020
Wing Mass [kg]	8722.4	+0.1%	8974 (+2.8%) ²
Workflow Time	-	<1day	<30 sec

¹: Calibrated on Reference data

²: Δ% respect to Ref Data

TAB 2. Multi-fidelity: Loads impact on sizing

Use Case D-150	Conceptual + Lo-Fi ^{3, 4}		
	1 LC	6 LC	+ gust LC
MTOM [kg]	74574.2	74986.1	77385
Fuel Mass [kg]	14972	15031.1	15138
OEM [kg]	40603	40955	43246
Wing Mass [kg]	6700 (-24%) ²	7034 (-19%) ²	9110 (+4.3%) ²
Workflow Time	<5 min	<5 min	<5 min

³: Converged valued of the OAD process (3-4 iterations full workflow), no calibration

⁴: Primary structures sized by Lo-Fi: strength + buckling constraints, only static

Comparing the results of the L0 conceptual synthesis with the reference, and the VAMP project, they are all very close. It has to be noted that both the conceptual system and the VAMP system, were calibrated against the reference values.

The results from the multi-fidelity approach refer to a fully converged synthesis (typically 3 or 4 fixed point iterations). The number of critical loads cases included for the structural sizing range from 1 (a representative 2.5 g maneuver), to 6 steady maneuvers within the design envelope, to 10 (which includes additional gust loads). The converged aircraft design masses show a difference between the L0 conceptual case, and the multi-fidelity which includes the physics based analysis. The main difference is in the operating empty mass (OEM) values, resulting by an under estimation of the computed structural masses. For a conventional configuration, conceptual design tools can provide very accurate results, since extensive database are available, and the synthesis process is calibrated on real aircraft data. On the other hand, physics based analysis would need to account for the simulation of a multitude of critical flight conditions and phenomena, to produce accurate results, without calibration factors. However, TAB 2 shows that increasing the critical loads cases has a mitigating effect, and physics design drivers are captured within acceptable time.

A second study is setup by adding the flexibility loop and the effects on the performance evaluation. In this case the representative number of sizing loads cases is reduced to 2. TAB 3 shows the results for the multi-fidelity with and without the flexibility loop enabled. For the rigid case the differences refer to the only conceptual L0 solution. Once more the under estimation of the structural component is stemming from the limited amount of critical conditions considered in the process. The reported flexible results show the differences of the synthesis with respect to the rigid case. For an aircraft featuring a conventional swept-back wing system with moderate aspect ratio, the structural flexibility is known to result into a degradation of the aerodynamics performance respect to the rigid analysis, as shown as well by the results in TAB 3. In fact the flexibility effect, when propagated through the OAD loop, generates an increase in fuel mass, and OEM in order to satisfy the defined TLAR

TAB 3. Multi-fidelity: Loads impact on flexible performance

Flexibility Effects	Conceptual + Lo-Fi	
	Δ ¹ Rigid %	Δ ² Flexible %
MTOM [kg]	-13%	+1.5%
Fuel Mass [kg]	-9%	+3%
OEM [kg]	-17%	+1%

¹: Δ% respect to Conceptual OAD values, 2 LC

²: Δ% respect to rigid OAD values, 2 LC

Both the studies show the impact the loads process has on the OAD synthesis at the early development stages. The impact is even larger for the investigation of unconventional configurations for which the conceptual design phase may not rely on an existing database. Hence, in order to capturing the major design drivers, physics based modules need to be included to unveil the driving phenomena.

3. SET-UP OF A STRUCTURAL MODEL FOR LOADS ANALYSIS FOR DLR-HALO

3.1. Research Aircraft DLR-HALO

The DLR HALO (High Altitude and LOng Range) Research Aircraft is an aircraft for atmospheric research and earth observation of the German science community. The HALO is based on a production G550 business jet from Gulfstream Aerospace Cooperation (GAC). For research purpose external wing stores at three stations per side can be supported by the DLR-HALO. The stores comprise pod, pylon, and hanger beam. All external stores require a separate certification. In order to strengthen the certification capabilities of DLR regarding the use of new wing pods, a specific DLR HALO loads process was established within the DLR project iLOADS. It is planned for the future to use such loads process to support the certification process for new wing pods, like the Particle Measurement System, the so-called PMS carrier (see FIGURE 6).



FIGURE 6. DLR-HALO with mounted PMS carrier

3.2. DLR HALO Data for the Structural Model and the Loads Analysis

Mandatory for a classical loads process is the use of representative structural models, comprising the stiffness characteristics of the aircraft and various mass configurations for a wide range of payload and fuel variants. As far as DLR lacks a structural model of the DLR HALO, several available reports and data from GAC and DLR that could contribute to the set-up of such model were taken into account. The structural model was planned to be realized as MSC Nastran finite element model.

Parts of the maintenance manual from GAC were used to model the load carrying structure of the wing-like structural components appropriately. Thus the wing and the tail structure are covered. Furthermore, GAC made a mass model for the minimum equipped weight (MEW) configuration available and center of gravity positions for various fuel conditions. Rules for the adding of mass items to the fuselage mass model were given as well. Regarding the loads, GAC provided DLR with the loads report used for the certification of the DLR HALO. The loads report contains a set of cutting loads of several

hundred load cases for representative station of the aircraft and the corresponding parameter for each load case (e.g. flight point, mass configuration, trim or gust analysis parameter). For the outer geometry of the DLR HALO a geometry model originally prepared for CFD calculations at DLR was used. Finally the results of the ground vibration test were taken to compare the structural dynamic characteristics of the structural model.

3.3. DLR-AE MONA Process

For the set-up of the structural model the DLR-AE MONA process was applied. MONA stands for the two main computer programs that are used in the process, ModGen and MSC Nastran. MONA is a combined loads and design process. The loads estimated in the first step are used for the application of various dimensioning methods like e.g. structural optimization with optimization algorithms to estimate the structural dimensions (e.g. wall thickness, area of stiffener elements) of each aircraft component.

ModGen is a DLR-AE in-house program to set up all simulation and optimization models for the loads analyses and the structural sizing of an aircraft component or the complete aircraft configuration. The model set-up is based on a parametric approach. This allows for the set-up of structural models where almost all structural parts are modelled according to the construction while a wide range of variations are still possible (e.g. outer geometry, construction concept). MSC Nastran is used for all simulation and the structural optimization task of the MONA process.

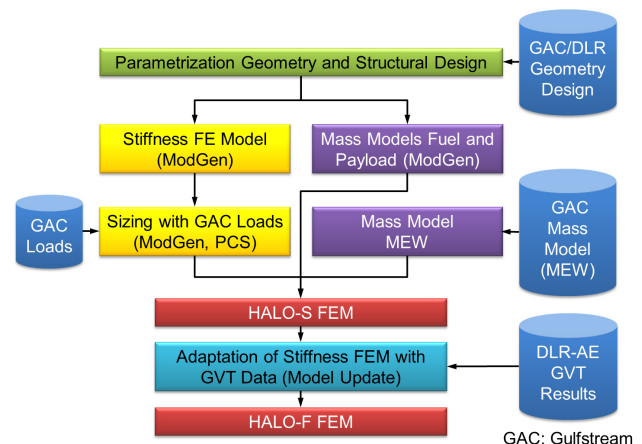


FIGURE 7. DLR-AE MONA process adapted to DLR-HALO

For the set-up of the structural model for the DLR HALO a modified MONA process is established as shown in FIGURE 7. The first step of MONA is the parametrization of the geometry and the structural design of each component with ModGen. Necessary data from GAC and DLR (e.g. geometry, construction concept) are taken into account. For the wing-like components the structural dimensions are estimated by a preliminary cross section sizing (PCS) method, an empirical-analytical method, using the available cutting loads from GAC (see also [3] and [9]). Transformed to the load reference axis coordinate system, the bending moment M_x , the torsion moment M_y , and the vertical force F_z are used to size the thickness of the skin, the spars, and the ribs as well as the dimensions of the stringer and the spar caps. Inner

stiffener elements of the spars and ribs were sized according to [22]. The fuselage is modelled with beam elements. For the sizing the method described in [1] is used. Therein the diameter of selected fuselage sections including the consideration of stiffener elements, like stringer, is taken into account. For the mass model on the one hand the MEW mass model from GAC is used. On the other hand the mass models for the fuselage payload and various fuel configurations are set up by DLR-AE. The distribution of the payload mass items is done according to the rules given by GAC in a mass report. The fuel mass modeling is done also with ModGen, where the individual filling levels and deck angles of the aircraft can be considered for each fuel tank.

3.4. DLR-HALO Finite Element Model

The resulting finite element model is shown in FIGURE 8a. For the loads analysis the structural model is condensed to selected nodes on the load reference axis (LRA) of each component (see FIGURE 8d). The condensation is based on the interpolation of the 6 degrees of freedom (DOFs) of the LRA grids by 6 selected DOFs of the fe grids of the full structural model shown in FIGURE 8a. Therefore the MSC Nastran element RBE3 with UM option is used. All distributed mass items (see FIGURE 8c) are also connected to the LRA grids. For the aerodynamics, a panel model for the Doublet Lattice Method (DLM) of MSC Nastran is set up by the MONA process where only the lifting surfaces are considered (see FIGURE 8b). In order to take wing twist and camber into account, corresponding correction factors are estimated by ModGen (MSC Nastran matrix W2GJ).

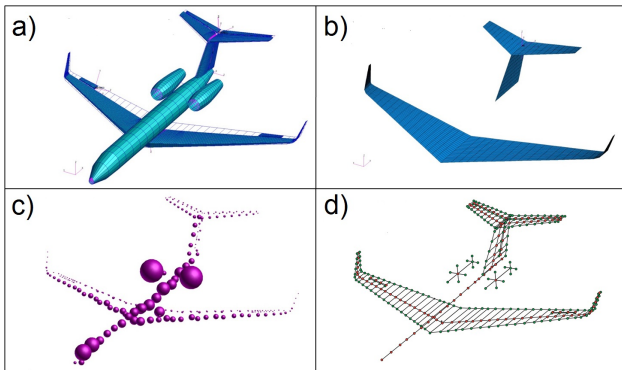


FIGURE 8. Finite element model HALO-S and aerodynamic model for DLM

The engine mass is connected to the fuselage beam with beam elements representing the pylon. The stiffness of the pylon beams is oriented to the results of the GVT test for the DLR HALO performed in 2009.

3.5. Results Loads Analysis

For the loads analysis various maneuver and gust load cases were selected from available GAC load data. The structural model was set up according to the given data. For the aircraft without fuel mass the mass and the center of gravity position are given. For the fuel configuration the fuel mass, the presumptive fuel distribution between the wing tanks and the deck angle of the aircraft are defined

as well. For defined flight conditions (e.g. altitude, Mach number, load factor) and trim conditions (horizontal tail with fixed angle, elevator angle is free trim variable), MSC Nastran SOL144 simulations were performed to estimate maneuver loads. The resulting bending moment M_x for the wing in spanwise direction is shown in FIGURE 9.

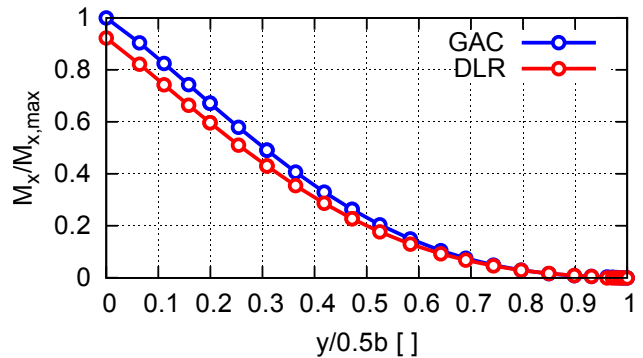


FIGURE 9. Normalized bending moment M_x for the wing for a 2.5 g symmetric maneuver load case

The maximum deviation of the estimated loads compared to the GAC loads for the specific load case is about 8% the average deviation about 3%. It is assumed that the differences are mainly caused by the aerodynamic model. A correction of the DLM model with spanwise available aerodynamic coefficients based on wind tunnel measurement were not yet taken into account. Furthermore the aerodynamic characteristics of the fuselage were not considered.

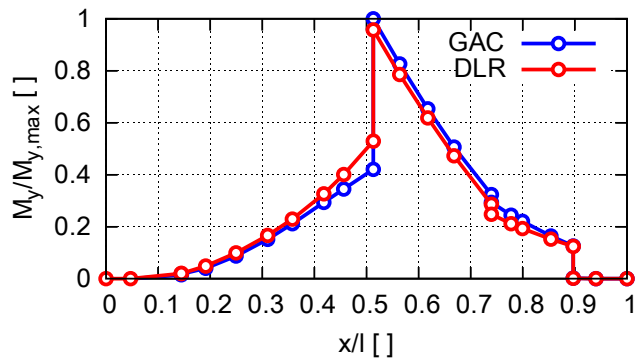


FIGURE 10. Normalized bending moment M_y along the fuselage for a 2.5 g symmetric maneuver load case

The resulting bending moment M_y along the fuselage is shown in FIGURE 10. The difference between the loads estimated with the MONA process and the GAC loads for the maximum load at the wing fuselage intersection is about 4%. The average difference for all monitor stations is about 2%. As preparation for the static tests of the PMS carrier mounted on the vibration table MAVIS of DLR-AE, a gust load analysis of a load case from GAC was performed with MSC Nastran Sol146. The simulation was done with the complete aircraft model with a wing pod mounted at the mid station. The time history of the displacements, velocities, and accelerations of a reference point near the LRA at the mid wing station was used as input signal for the MAVIS to simulate vibrations acting on the PMS carrier that are caused by a gust encounter.

4. LOADS FLIGHT TESTING WITH DLR HALO

In April 2016 five test flights with DLR HALO were carried out at the DLR site Oberpfaffenhofen, with around 13 flying hours in total. The aims were to collect flight loads measurement data at the wingpods to validate DLR simulation methods for loads analysis and to investigate the aircraft oscillations in flight using an online monitoring system. The latter is described further in the paper by Sinske [19]. The utilized wingpods are PMS (Particle Measurement System) carriers which are mounted on the middle wing station on each side of the wing, as shown in FIGURE 11.



FIGURE 11. PMS carrier mounted on the wing station

4.1. Gust simulation on the vibration table MAVIS

One preliminary test for the flight experiment was a gust simulation of the PMS carrier at DLR in Göttingen. For this aim the PMS carrier was mounted upside down on the vibration table MAVIS (Mehrachsen-Vibrationssimulator, multi axis vibration simulator). The setup is illustrated in FIGURE 12. The gust load case selected for the simulation is a design load case for the PMS carrier, with a gust gradient of 50 feet (16 m). In order to generate the input signal for the MAVIS, a numerical gust simulation with models explained in section 3 was performed beforehand. In the numerical simulation the PMS carrier was represented by rigid bodies and the hanger beam by an elastic beam. The results in form of deflection, velocities and accelerations were extracted, scaled down and taken as inputs for the gust simulation on the MAVIS. The time history of the hardpoint displacement resulting from the numerical simulation is depicted in FIGURE 12.

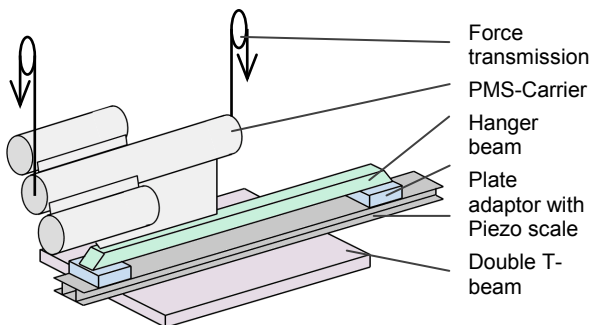


FIGURE 12. Strain gage calibration setup on vibration table MAVIS

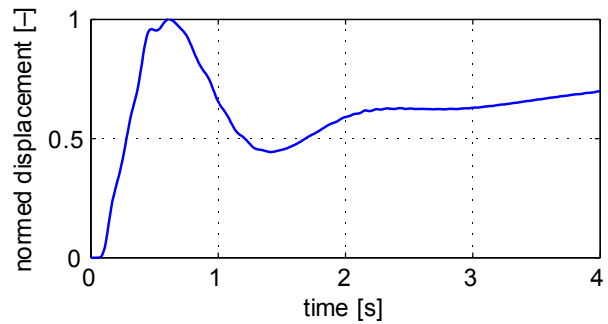


FIGURE 13. Time history of the normed hardpoint displacement from a numerical gust simulation

4.2. Strain gage calibration and pre-flight tests

The flight loads measurement for the PMS carrier is performed with strain gages [19] [20]. The calibration of the strain gages is done by applying linearly independent loads on the PMS carrier and measuring the strain signals. With sufficient applied loads – more than the number of bridges – the relation between load and strain signal can be identified which enables the calculation of loads based on strain signals [20].

The first calibration of the strain gages was carried out at DLR in Göttingen. The load application was conducted with the help of sandbags. Weights up to 50 kg were attached to each force transmission point. To minimize error due to hysteresis, the applied loads were increased and decreased step by step. The strain signals were measured for each step. A typical strain response of a two-step load case is shown in FIGURE 14.

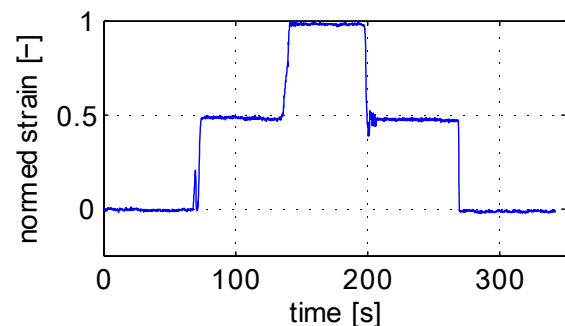


FIGURE 14. Typical strain response of a two-step load application

The second calibration of the strain gages was performed at DLR in Oberpfaffenhofen where both PMS carriers were mounted on the wing station of the DLR HALO. In total nine linearly independent loads were applied on each PMS carrier, and transfer matrices to calculate loads from strain signals were derived. A picture of load application during the calibration is presented in FIGURE 15.

In addition, an electromagnetic compatibility test and a taxi vibration test were carried out beforehand to ensure the functionality and the safety of the measurement systems in flight [19].



FIGURE 15. Strain gage calibration for one PMS carrier

4.3. Flight tests

The second flight was conducted for loads measurement, where several maneuvers were flown for different conditions. In total there are 21 flight conditions consisting of seven altitudes ranging from 12000 ft to 35000 ft (3658 m to 10668 m) and three speeds each. The maneuvers for each flight condition consist of impulsive inputs on the yoke and rudder pedals, a roll up to $\pm 45^\circ$ and a pull-up up to 2 g.

The initial aim was to simulate gust loads using maneuvers since gust loads are design loads for the hardpoints where the hanger beam is mounted. However, to do so stick raps with a frequency of up to 14 Hz would be necessary. Such procedure is difficult to perform with high precision. Furthermore, the control surface actuation system filters the high frequency input to some degree. Instead, impulsive inputs on the steering system and low frequent maneuvers as described above were considered as safer and easier to perform. A time history of the load factor during a pull-up maneuver is presented in FIGURE 16.

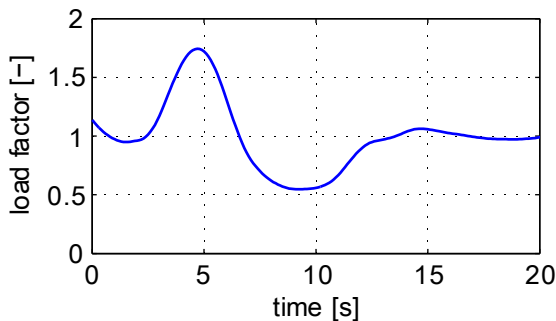


FIGURE 16. Load factor during a pull-up maneuver

A normed strain signal response of the left hand side PMS carrier with all eight channels during a roll maneuver is depicted in FIGURE 17. It is evident that the strain response is already detectable before the bank angle

increases. This indicates that the strain reacts in phase with the roll acceleration. A further investigation of the loads based on strain responses is still to be done.

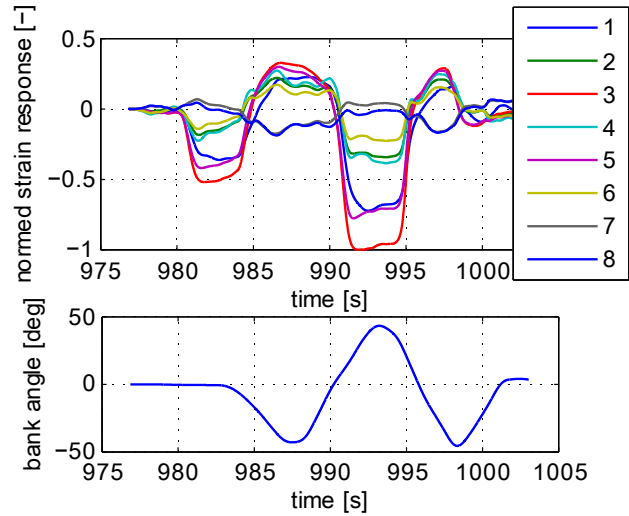


FIGURE 17. Normed strain signal response during a roll maneuver

Beside strain responses, atmospheric turbulence data was also collected during the flights. Its first analyses in the frequency domain show that the power spectral density of the measured turbulence is similar to a von-Kármán spectrum [7], however with a smaller scale of turbulence than 2500 ft (762 m) which is defined in CS25 [14]. A smaller scale of turbulence means that more energy of the turbulence is contained in oscillations with higher frequencies. An example of the power spectral density of the measured turbulence and reference von-Kármán spectra are depicted in FIGURE 18, where L stands for the scale of turbulence. With this finding, loads analysis methods regarding atmospheric turbulence can be improved for the future.

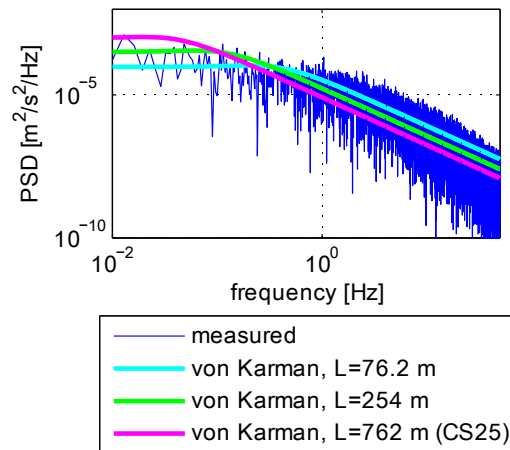


FIGURE 18. Power spectral density of measured turbulence in comparison with reference von-Kármán spectra

5. SYSTEM IDENTIFICATION FOR DLR DISCUS 2C

This iLOADS work package focuses on the development of real time capable rigid-body and flexible multipoint loads models based on flight test data using System-Identification in time domain [8]. As test aircraft the new DLR Discus-2c sailplane was used (see FIGURE 19). In addition to a basic flight test instrumentation including IMU, nose boom with 5-hole probe and control surface deflection sensors several strain sensors and accelerometers within wing, fuselage and horizontal tail were installed already during the aircraft construction. The strain sensors were calibrated in an extended ground test campaign to enable local loads measurements [23]. These direct loads measurements at different positions of the aircraft structure were used to extend the typical set of observation variables for enabling the prediction of local aerodynamic loads. For this purpose a flight test program with 22 flights and specific maneuvers covering low and high frequency control inputs at different airspeeds was performed. In this context, the System-Identification approach is briefly explained and some exemplary results are presented.



FIGURE 19. DLR Discus-2c flight test sailplane [17]

5.1. System-Identification Approach

The conventional System-Identification uses flight data as input in order to model the aircraft aerodynamic loads. However, due to the limited information provided by the standard flight test instrumentation only the global aerodynamic contributions of wing/fuselage and horizontal tail can be modeled. The objective of this work was to extend the model for providing the capability to simulate local loads at certain positions of wing, horizontal tail and fuselage. However, this multipoint loads modeling requires the availability of local loads measurements as additional observation variables to provide sufficient information for the identification of a significant number of model parameters. FIGURE 20 shows the wing and horizontal tail cutting loads available at 7 stations after calibrating the overall 46 strain sensors. The notation S, B and T means shear force, bending moment and torque respectively. By subtracting the structural inertia masses from the loads measurements local aerodynamic lift (C_L), pitching (C_m) and rolling moment (C_l) coefficients for each wing segment and horizontal tail were calculated. C_{LWR6} for example is the lift coefficient for the right wing segment from the WR6 load station to the wing tip. For the development of a 7-point flight mechanical model these measured local aerodynamic coefficients were used like shown in the System-Identification scheme in FIGURE 21 for finding the best match between measurement and model the DLR software FITLAB [5] was used to estimate the model parameter values. More detailed descriptions of the model structure and the identified parameter values can be found in [25] and [24].

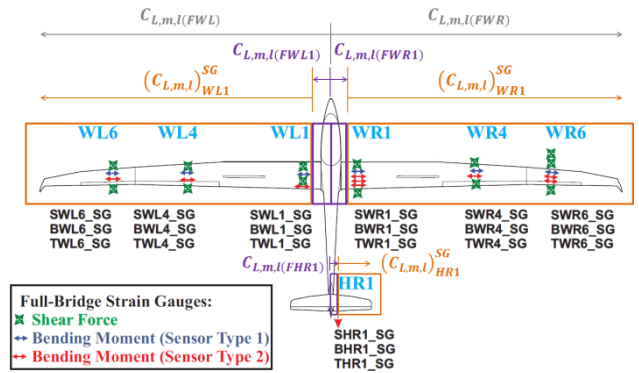


FIGURE 20. Structural and aerodynamic loads calculated from 46 strain gauge measurements [1]

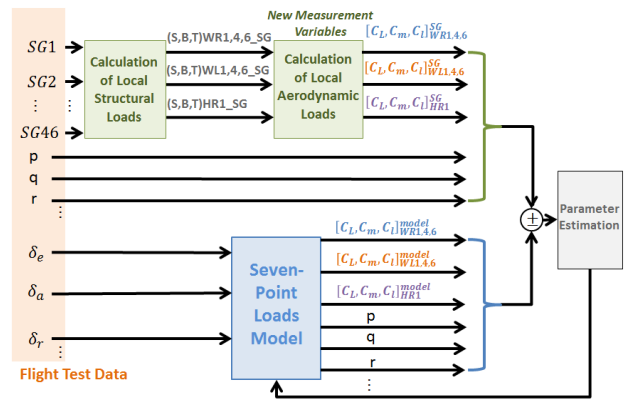


FIGURE 21. System-Identification scheme of 7-point loads model

5.2. Results

The following FIGURE 22 and FIGURE 23 show some exemplary System-Identification results for typical longitudinal and lateral flight test maneuvers. Therefore the time histories show model outputs (red lines) in comparison to the flight test data (blue lines). The first 8 plots show control surface deflections and main aircraft motion parameters like speed, angles of attack and sideslip and rotation rates p , q , r . The next 7 plots show the local aerodynamic lift coefficients for 6 wing segments and horizontal tail.

FIGURE 22 depicts a stall approach maneuver combined with a sequence of elevator doublets. This provides flight data that cover a large angle of attack, pitch rate and elevator deflection range. It can be observed that the identified 7-point loads model presents a good agreement with the measured local aerodynamic loads along the entire angle of attack range. Additionally, these results show the efficacy of the implemented stall model used to account for the wing lift-curve slope reduction at high angles of attack. For analyzing the longitudinal-lateral-degrees-of-freedom coupling effects and its influence on the local loads, several types of flight maneuvers were applied to the System-Identification process. One example is the 3-2-1-1 aileron multistep input shown in FIGURE 23. It can be observed that the peaks of the local spanwise lift coefficient along the wing relate directly to the aileron excitations. Overall a very good matching between flight test and simulation model is achieved.

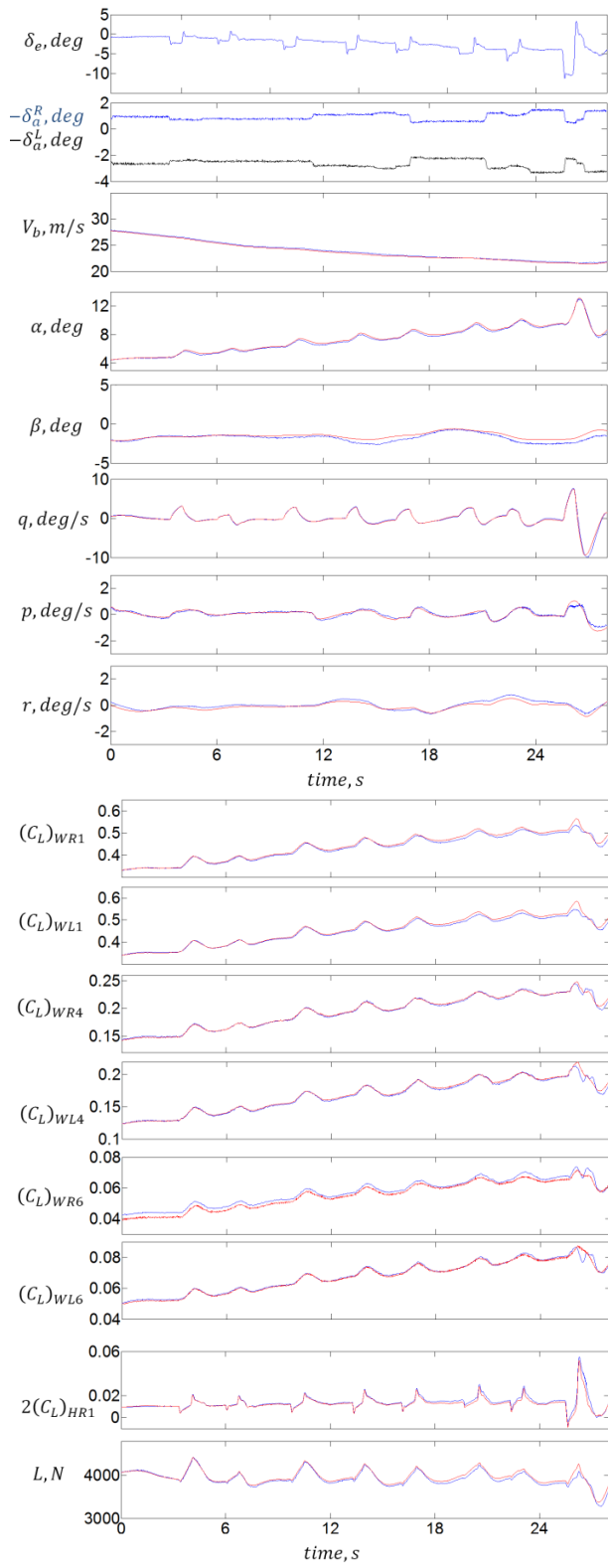


FIGURE 22. Comparison Measurement – Model: Stall approach combined with elevator doublets

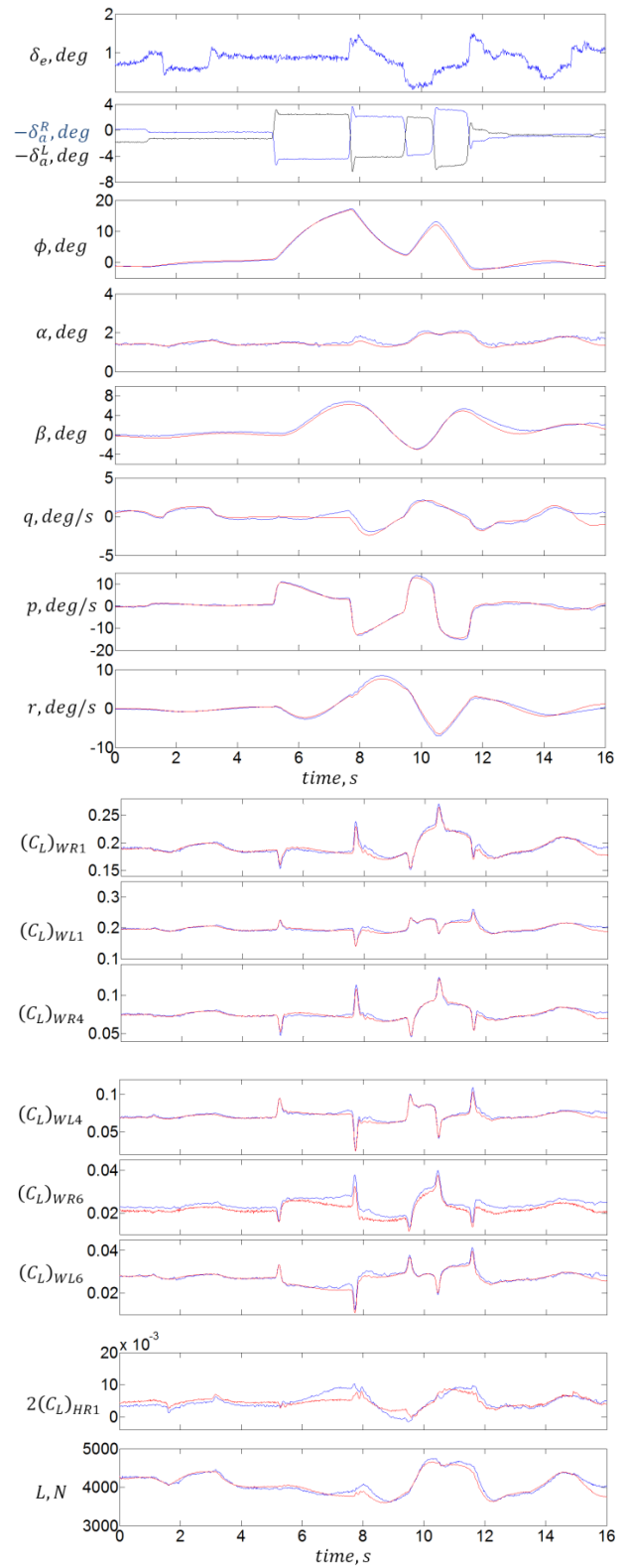


FIGURE 23. Comparison Measurement – Model: 3-2-1-1 aileron multistep inputs

6. SUMMARY

The use case work package of the DLR project iLOADS showed the wide range of loads analysis from conceptual design to loads flight testing.

For conceptual design a physics base loads and sizing process is presented as part of a typical overall aircraft design process, where normally statistics based or analytical methods are applied. Furthermore the flexibility of the structure was not only considered for the structural sizing, but also for the aerodynamic performance analysis.

Regarding the loads analysis for a complete aircraft, a parametric loads and design process is outlined and applied to the DLR HALO. The set-up of a proper structural model with the MONA process is shown as well as the analysis of selected load cases to be compared to results from GAC. In order to measure the interface loads between the store and the wing of the HALO with mounted PMS carrier, the structural model is also used to simulate gust analysis. The results serve as input for pre-tests on the vibration table MAVIS. Eventually first results of the measured flight loads are shown.

Finally first results for a loads model for the DLR Discus-2c based on flight test is shown. Two test campaigns of the considerably equipped sailplane with various sensors are a basis not only for a loads model, but for an overall system identification of the aircraft.

SCHRIFTTUM

- [1] M. D. Ardema, M. C. Chambers, A. P. Patron, A. S. Hahn, H. Miura, and Mark D. Moore. Analytical fuselage and wing weight estimation of transport aircraft. Technical Report Technical Memorandum 110392, NASA, May 1996.
- [2] P. D. Ciampa, T. Zill, and B. Nagel. A hierarchical aeroelastic engine for the preliminary design and optimization of the flexible aircraft. In *In Proceedings of 54th AIAA/ASME/ASCE/AHS/ASC Structures, Structural Dynamics, and Materials Conference, April 8-11, 2013, Boston, Massachusetts*, number AIAA 2013-1820, 2013.
- [3] F. Van Dalen. MDO load analysis and preliminary sizing. Technical report, Delft University of Technology, December 1996.
- [4] M. J. de C. Henshaw, K.J. Badcock, G.A., Vio, C.B. Allen, J. Chamberlain, I. Kaynes, G. Dimitriadis, J.E. Cooper, M.A. Woodgate, A.M. Rampurwala, D. Jones, C. Fenwick, A.L. Gaitonde, N.V. Taylor, D.S. Amor, T.A. Eccles, and C.J. Denley. Non-linear aeroelastic prediction for aircraft applications. *Progress in Aerospace Sciences*, 43:65–137, May-Aug 2007.
- [5] DLR - German Aerospace Center. CPACS - Common Parametric Aircraft Configuration Schema, Sept. 2016. www.cpacs.de (last checked 2016-09-12).
- [6] DLR - German Aerospace Center. RCE - Remote Component Environment, Sept. 2016. www.rcenvironment.de (last checked 2016-09-12).
- [7] F. M. Hoblit. *Gust Loads on Aircraft: Concepts and Applications*, volume ISBN 0-930402-45-2 of *AIAA Education Series*. AIAA, 1988.
- [8] R. V. Jategaonkar. Flight Vehicle System Identification: A Time Domain Methodology. *Progress in Astronautics and Aeronautics*, 216, 2006. Reston, VA, USA.
- [9] T. Klimmek. *Statische aeroelastische Anforderungen beim multidisziplinären Strukturentwurf von*

Transportflugzeugflügeln. Dissertation, TU-Braunschweig, August 2016. DLR-FB 2016-34.

[10] W. Krüger and T. Klimmek. Definition eines übergreifenden Lastenprozesses im DLR-Projekt iLOADS. In *Deutscher Luft- und Raumfahrtkongress, 13-15 Sept 2016, Braunschweig (Germany)*, 2016.

[11] T. L. Lomax. *Structural Loads Analysis for Commercial Transport Aircraft: Theory and Praxis*. Number ISBN 1-56347-114-0. AIAA Education Series, 1996.

[12] B. Nagel, T. Zill, E. Moerland, and D. Böhnke. Virtual Aircraft Multidisciplinary Analysis and Design Processes – Lessons Learned from the Collaborative Design Project VAMP. In *in Proceedings of 4th CEAS Air & Space Conference, 16-19 Sep., Linköping, Sweden*, 2013.

[13] M. Niu. *Airframe Stress Analysis and Sizing*. Number ISBN-13: 978-9627128120. Hong Kong Conmillit Press LTD, Hong Kong, 1999.

[14] N.N. *CS25 - Certification Specifications and Acceptable Means of Compliance for Large Aeroplanes*. <http://easa.europa.eu/document-library/certification-specifications/cs-25-amendment-14>, last checked 2014-05-20 2013. Amendment 14.

[15] D.P. Raymer. *Aircraft Design: A Conceptual Approach*. AIAA Education Series, Washington, DC, 1989. ISBN 0-930403-51-7.

[16] J. R. Wright and J. E. Cooper. *Introduction to Aircraft Aeroelasticity and Loads*. Number ISBN 978-0470-85840-0. Wiley, 2007.

[17] Schempp-Hirth Flugzeugbau GmbH, Kirchheim unter Teck, Germany. *Flughandbuch für das Segelflugzeug Discus-2c*, 2005. (in German).

[18] D. Seider, P. M. Fischer, M. Litz, A. Schreiber, and A. Gerndt. Open source software framework for applications in aeronautics and space. In *in Proceedings of IEEE Aerospace Conference, 3-10 March 2012, Big Sky, Montana, USA*, 2012.

[19] J. Sinske, Y Govers, V. Handojo, and W.-K. Krüger. HALO Flugtest mit instrumentierten Außenlasten für Aeroelastik- und Lastmessungen im DLR-Projekt iLOADS. In *Deutscher Luft- und Raumfahrtkongress 2016, 13-16 Sept. 2016, Braunschweig*. DGLR, 2016. (to be published).

[20] T.H. Skopinski, Aiken Jr., W.S., and W.B. Huston. Calibration of strain-gage installations in aircraft structures for the measurement of flight loads. Technical Report NACA Report No. 1178, NACA, 1954.

[21] E. Torenbeek. *Synthesis of Subsonic Airplane Design*. Delft University Press, Delft, 1988. ISBN 90-247-2724-3.

[22] F. van Dalen and A. Rothwell. Adas structures module: User's manual. Memorandum M-709, TU-Delft, 1995.

[23] M. V. Preisighe Viana. Sensor calibration for calculation of loads on a flexible aircraft. In *16th International Forum on Aeroelasticity and Structural Dynamics - IFASD 2015, 28 June - 2 July 2015, Saint Petersburg, Russia*, 2015.

[24] M. V. Preisighe Viana. *Multipoint Loads Model for Flexible Aircraft Health Monitoring in Real Time*. Dissertation, Institut für Flugsystemtechnik, 2016. (to be published).

[25] M. V. Preisighe Viana. Time-domain system identification of rigid-body multipoint loads model. In *American Institute of Aeronautics and Astronautics (AIAA), Atmospheric Flight Mechanics Conference, June 2016, Washington D.C., USA*, 2016.